Integrating Machine Learning and Traditional Survival Analysis to Identify Key Predictors of Foveal Involvement in Geographic Atrophy

Maria Vittoria Cicinelli,[1,2] Eugenio Barlocci,[1,2] Chiara Giuffrè,[2] Federico Rissotto,[1,2] Ugo Introini,[2] and Francesco Bandello[1,2]

[1]School of Medicine, Vita-Salute San Raffaele University, Milan, Italy
[2]Department of Ophthalmology, IRCCS San Raffaele Scientific Institute, Milan, Italy

Correspondence: Maria V. Cicinelli, Department of Ophthalmology, IRCCS San Raffaele Scientific Institute, Via Olgettina 60, Milan 20132, Italy;
cicinelli.mariavittoria@hsr.it.

Received: January 20, 2024
Accepted: April 17, 2024
Published: May 6, 2024

Citation: Cicinelli MV, Barlocci E, Giuffrè C, Rissotto F, Introini U, Bandello F. Integrating machine learning and traditional survival analysis to identify key predictors of foveal involvement in geographic atrophy. *Invest Ophthalmol Vis Sci.* 2024;65(5):10.
https://doi.org/10.1167/iovs.65.5.10

Purpose. The purpose of this study was to investigate the incidence of foveal involvement in geographic atrophy (GA) secondary to age-related macular degeneration (AMD), using machine learning to assess the importance of risk factors.

Methods. Retrospective, longitudinal cohort study. Patients diagnosed with foveal-sparing GA, having GA size $\geq$ 0.049 mm^2 and follow-up $\geq$ 6 months, were included. Baseline GA area, distance from the fovea, and perilesional patterns were measured using fundus autofluorescence. Optical coherence tomography assessed foveal involvement, structural biomarkers, and outer retinal layers thickness. Onset of foveal involvement was recorded. Foveal survival rates were estimated using Kaplan-Meier curves. Hazard ratios (HRs) were assessed with mixed model Cox regression. Variable Importance (VIMP) was ranked with Random Survival Forests (RSF), with higher scores indicating greater predictive significance.

Results. One hundred sixty-seven eyes (115 patients, average age = 75.8 $\pm$ 9.47 years) with mean follow-up of 50 $\pm$ 29 months, were included in this study. Median foveal survival time was 45 months (95% confidence interval [CI] = 38–55). Incidences of foveal involvement were 26% at 24 months and 67% at 60 months. Risk factors were GA proximity to the fovea (HR = 0.97 per 10-µm increase, 95% CI = 0.96–0.98), worse baseline visual acuity (HR = 1.37 per 0.1 LogMAR increase, 95% CI = 1.21–1.53), and thinner outer nuclear layer (HR = 0.59 per 10-µm increase, 95% CI = 0.46–0.74). RSF analysis confirmed these as main predictors (VIMP = 16.7, $P = 0.002$; VIMP = 6.2, $P = 0.003$; and VIMP = 3.4, $P = 0.01$). Lesser baseline GA area (HR = 1.09 per 1-mm^2 increase, 95% CI = 1.01–1.16) and presence of a double layer sign (HR = 0.42, 95% CI = 0.20–0.88) were protective but less influential.

Conclusions. This study identifies anatomic and functional factors impacting the risk of foveal involvement in GA. These findings may help identify at-risk patients, enabling tailored preventive strategies.

Keywords: geographic atrophy (GA), age-related macular degeneration (AMD), foveal involvement, machine learning, random survival forests (RSF)

Geographic atrophy (GA), the advanced and irreversible stage of age-related macular degeneration (AMD), significantly compromises vision and quality of life.[1] In its early phases, GA often spares the fovea, allowing patients to maintain relatively good visual acuity (VA). However, as GA involves the fovea, it inevitably leads to profound and irreversible central vision loss.[2] This critical phase not only marks a significant escalation in the disease's severity but also serves as a key prognostic marker. The use of optical coherence tomography (OCT) is indispensable in this context, providing high-resolution images that accurately assess the extent and the progression of retinal pigment epithelium (RPE) and outer retinal atrophy (cRORA).[3]

Emerging treatments, notably intravitreal complement inhibitors, although unable to reverse neurosensory retinal cell loss, can decelerate photoreceptor loss adjacent to GA borders.[4,5] This development highlights the necessity of promptly identifying patients at risk of foveal involvement to optimize stratification and treatment allocation effectively. However, the inherent diversity in GA's clinical presentation poses significant challenges in developing uniform treatment approaches and predicting disease progression on an individual basis.[6]

Coping with the complex nature of GA manifestations, our research uses a machine learning method by applying the Random Survival Forest (RSF) algorithm to explore the incidence and risk factors of foveal involvement

in patients with initial foveal-sparing GA. This approach complements traditional survival analysis methods like Cox regression, which primarily yields coefficients indicating variable effects. Our application of RSF addresses a gap in current research by introducing Variable Importance Measures (VIMP) for each risk factor.

The use of both approaches significantly advances our understanding of GA prognosis, ranking candidate risk factors not only by their impact but also by their importance.[7] By doing so, this research aspires to enhance clinical decision-making processes, highlighting patients who would most benefit from proactive and tailored interventions to mitigate the progression of GA.

Methods

This retrospective, longitudinal study was undertaken at the San Raffaele Scientific Institute, Milan, Italy, spanning from April 2011 to November 2023. The chosen timeframe ensured uniformity in imaging techniques, as all patients with AMD were examined using the same OCT device throughout this period. Conducted in line with the Declaration of Helsinki, the study protocol received an exemption from requiring written informed consent by the local institutional review board.

The study enrolled participants aged 50 years and above, diagnosed with non-exudative AMD. Eligibility criteria included a minimum GA area of 0.049 mm^2, equivalent to a circle diameter of approximately 250 µm, located within 800 µm of the fovea. This area of GA was required to be situated within the inner circle of an Early Treatment Diabetic Retinopathy Study (ETDRS) grid. Fovea-sparing was specifically defined as the presence of a residual foveal island larger than 270 degrees.[8] We excluded individuals who presented with foveal involvement at their initial visit, those with any form of macular neovascularization (MNV), other retinal diseases, or those who had undergone prior ocular treatments. A minimum follow-up duration of 6 months was established for the study. In cases where both eyes of a patient met the inclusion criteria, data from both eyes were included in the analysis.

Data Collection and Imaging

Chart reviews were performed and data on demographics, ophthalmic history, and the fellow eye were collected for baseline visits (i.e. the first visit that satisfied the inclusion criteria). At each following visit, VA was originally assessed using ETDRS tables and then converted to LogMAR for analysis. Confocal scanning laser ophthalmoscopy (cSLO) was used to perform blue-light fundus autofluorescence (FAF) imaging across the central 30 degrees of the retina. Additionally, a series of six radial scans were acquired using spectral-domain OCT (SD-OCT), utilizing eye tracking and follow-up modes on the Spectralis HRA+OCT system (Heidelberg Engineering, Heidelberg, Germany). The selection of any supplementary imaging methods was left to the discretion of the attending ophthalmologist.

The analysis of these baseline FAF and SD-OCT images was conducted by two experienced ophthalmologists (authors E.B. and C.G.), who were masked to the outcomes of the study. Expert adjudication was provided by a retina specialist (author M.V.C.) in cases of disagreement. The FAF patterns surrounding GA areas were classified into: none, focal, diffuse (with further differentiation into subtypes such as reticular, branching, granular, and trickling), banded, or patchy.[9] The RegionFinder software was used to measure the GA area on FAF at baseline, confirmed by near-infrared imaging co-registered with SD-OCT.

Qualitative and Quantitative SD-OCT Measurements

Qualitative SD-OCT assessments included identification of subretinal drusenoid deposits (SDD; $\geq$ 3 lesions identified on one B-scan),[10,11] refractile drusen ($\geq$ 1 lesion identified on one B-scan),[12] and the double layer sign (DLS).[13,14] DLS exceeding 1000 µm in length and 100 µm in height on horizontal B-scan, or exhibiting multiple reflective layers between the RPE and the Bruch's membrane (BM), were excluded to mitigate the risk of confounding by non-exudative MNV.

Criteria for foveal involvement were defined as choroidal signal hypertransmission with RPE disruption and photoreceptor degeneration in the 1-mm central area beneath the foveal depression, extending over a width of more than 250 µm on the horizontal B-scan.[3] The occurrence date of the initial foveal involvement was recorded by the graders.

Quantitative analyses included the calculation of thickness for the outer nuclear layer (ONL) and the entirety of the outer retinal layer, spanning from BM to the external limiting membrane, within the central 1-mm diameter of the ETDRS map. The thickness measurements were automatically derived using the Spectralis software, complemented by manual segmentation adjustments when necessary. Additionally, manual measurements were taken to determine the vertical thickness of the choroid beneath the foveal depression, as well as the maximal elevation of the DLS on corresponding B-scans. The agreement between the two graders, measured on a subset of 10 B-scan, was excellent, with an intraclass correlation coefficient (ICC) of 0.98 for choroidal thickness and 0.95 for the maximal elevation of the DLS.

The minimum distance between the GA region and the fovea was also manually determined, using near-infrared imaging.

Statistical Analysis

Statistical analyses were conducted using the R programming environment. Continuous variables were summarized either as mean $\pm$ standard deviation or as median and interquartile range (IQR). Categorical variables were presented as counts and percentages.

To estimate the incidence of foveal involvement, the Kaplan-Meier survival method was applied. This analysis included censoring cases that did not exhibit foveal involvement or were lost to follow-up at their last known visit. In instances where MNV developed post-baseline, follow-up was truncated at its onset.

For identifying risk factors associated with the progression to foveal involvement, a multivariable Cox regression model was used. This involved utilizing penalized maximum likelihood estimation through the *glmnet*[15] package, with the elastic net mixing parameter α set to 1, indicative of lasso regularization. Model optimization was achieved via 10-fold cross-validation to determine the most appropriate

Investigative Ophthalmology & Visual Science

lambda value. A mixed model was integrated to account for inter-eye correlations in cases of bilateral involvement. The model provided hazard ratios (HRs) and their respective 95% confidence intervals (CIs) for each variable. To affirm the robustness and validity of the Cox model, a proportional hazards assumption test was conducted using the *cox.zph* function, and diagnostic plots focusing on dfbeta values were generated via the *ggcoxdiagnostics* function to identify and exclude influential cases potentially skewing the model's estimates.

Further analysis of risk factors used the RSF method, implemented via the *randomForestSRC* package. This approach entailed the construction of decision trees for data subsets, each generated from a bootstrap sample,[16] with the log-rank test statistic as the default splitting rule. Approximately 37% of the dataset, classified as out-of-bag (OOB) instances, were excluded from each tree's training set and used for validation purposes. The RSF model parameters, including the number of trees (B = 1500) and the number of split candidate features at each node (m = 5), were optimized through a 5 × 5-fold cross-validation process. The node size parameter, indicative of the minimum number of distinct instances required in a terminal node, was set at 3, acting as a pruning mechanism. The model's efficacy was evaluated using VIMP, with VIMP calculated as the difference between the average perturbed and original OOB prediction error. The patient ID was incorporated as a cluster variable in our model to account for intrapatient correlations.

Partial Dependence Plots (PDPs) were used to visualize the relationship between key predictors and the likelihood of progression toward foveal involvement at the median follow-up time of 46 months. Prior to the analysis, predictors were standardized (z-scores) to ensure comparability across different scales, transforming each variable to have a mean of 0 and a standard deviation of 1. This standardization facilitated the assessment of how deviations from the mean influenced survival probabilities, independent of the units or magnitude of original measurements. Dummy variables were created for categorical data and missing data (Supplementary Fig. S1) were imputed using the mean of available data.

The RSF analysis was conducted on a training set that comprised 70% of the instances (116 eyes) and validated on the remaining 30% set (51 eyes).

Results

This study evaluated 167 eyes from 115 patients diagnosed with non-exudative AMD, presenting with foveal-sparing GA. Most participants (75%) contributed with one eye as the fellow eye had already foveal-involving GA or exudative AMD. Over the median follow-up of 46 months (IQR = 28.5 to 66), 59% (98 eyes) progressed to foveal involvement (Table 1).

The participants' ages ranged from 50 to 94 years, with the group maintaining fovea sparing being slightly older on average (75.8 ± 9.47 years) compared to the group progressing to foveal involvement (74.0 ± 9.65 years). Female subjects constituted the majority of the cohort (70.1%). Baseline VA was generally better in the foveal sparing group (0.217 ± 0.204 LogMAR) than in the foveal involvement group (0.303 ± 0.305 LogMAR), although both groups exhibited considerable variability. The pattern of GA was predominantly multifocal (68%), with "diffuse" being the most FAF frequent pattern. The average baseline GA area measured 3.87 mm^2, with a greater average distance from the fovea in the foveal sparing group (563 ± 265 µm) compared to the foveal involvement group (382 ± 304 µm).

Incidence of Foveal Involvement and Risk Factors

The median time to foveal involvement was 45 months (95% CI = 38–55 months). Kaplan-Meier estimates indicated increasing incidence over time: 14% at 12 months, 26% at 24 months, 40% at 36 months, and 67% at 60 months (Fig. 1).

The multivariable Cox mixed-effects model identified several significant risk factors after excluding irrelevant variables with lasso regression, which are listed in Table 2. Each 10 µm increase in the distance of GA from the fovea reduced the risk of foveal involvement by 3% (HR = 0.97, 95% CI = 0.96–0.98, $P < 0.001$). Each 1 mm^2 increase in baseline GA area raised the risk by 8.5% (HR = 1.085, 95% CI = 1.01–1.16, $P = 0.02$) and each 0.1 increase in LogMAR VA increased the risk by 37% (HR = 1.37, 95% CI = 1.21–1.53, $P < 0.001$). A thicker ONL was protective (HR = 0.59 per 10-µm increase, 95% CI = 0.46–0.74, $P < 0.001$), whereas increased outer retinal layer thickness heightened risk (HR = 1.70 per 10-µm increase, 95% CI = 1.11–2.59, $P = 0.01$). The presence of DLS (HR = 0.42, 95% CI = 0.20–0.88, $P = 0.02$) and SDD presence were protective factors (HR = 0.39, 95% CI = 0.18–0.84, $P = 0.02$).

There was substantial variation in baseline risk among patients, as indicated by the random effects' standard deviation (1.16), pointing to the significant influence of individual patient characteristics on the risk of foveal involvement not accounted for by the fixed effects in our model. Furthermore, the comparison of model fits, as evidenced by the Akaike Information Criterion (AIC), favored the nested model incorporating patient ID over the simple effect model. With a lower AIC of 618 compared to 653 in the simple model (ANOVA P value = 0.01), the nested model highlights the importance of considering intra-individual variability in foveal involvement in GA.

Random Survival Forests Analysis and Risk Factors Importance

The RSF analysis identified critical predictors of foveal involvement in patients with GA. A representative regression tree, randomly chosen from the 1500 trees generated, illustrates these findings in Supplementary Figure S2.

The distance from the fovea was the most significant predictor, with VIMP of 16.7 ($P = 0.002$). Baseline VA followed in importance, with a VIMP of 6.2 ($P = 0.003$). The ONL thickness was also a key factor, having a VIMP of 3.35 ($P = 0.01$). The RSF analysis also highlighted the significance of the thickness of the outer retinal layers, which displayed a VIMP of 1.85 ($P = 0.01$). Interestingly, partial dependence plots revealed a bi-phasic relationship between this factor and the risk of foveal involvement (see Figure 2B, Supplementary Table S1). Additionally, the presence of a focal FAF pattern was identified as an influential factor with a VIMP of 1.85 ($P = 0.02$), linked to a higher risk of foveal involvement.

The comparison of the results between the training and the validation set is shown in Supplementary Figure S3.

Investigative Ophthalmology & Visual Science

Table 1. Demographic and Clinical Characteristics of the Study Population, Categorized Based on the Presence of Foveal Sparing (69 Eyes) and Foveal Involvement (98 Eyes), With Overall Data for all 167 Eyes With Geographic Atrophy (GA), Included in the Study

	Foveal Sparing ($N = 69$ Eyes)	Foveal Involvement ($N = 98$ Eyes)	Overall ($N = 167$ Eyes)
Age, y			
Mean (SD)	75.8 (9.47)	74.0 (9.65)	74.8 (9.59)
Median [min, max]	77.0 [51.0, 94.0]	76.0 [50.0, 89.0]	76.0 [50.0, 94.0]
Gender			
M	17 (24.6%)	31 (31.6%)	48 (28.7%)
F	50 (72.5%)	67 (68.4%)	117 (70.1%)
Baseline visual acuity (LogMAR)			
Mean (SD)	0.217 (0.204)	0.303 (0.305)	0.268 (0.270)
Median [min, max]	0.150 [0, 1.00]	0.220 [0, 1.30]	0.220 [0, 1.30]
GA focality			
Multifocal	45 (65.2%)	68 (69.4%)	113 (67.7%)
Unifocal	24 (34.8%)	30 (30.6%)	54 (32.3%)
Pattern			
None	1 (1.4%)	3 (3.1%)	4 (2.4%)
Diffuse	53 (76.8%)	73 (74.5%)	126 (75.4%)
• Reticular	34 (49.3%)	41 (41.8%)	75 (44.9%)
• Trickling	12 (17.4%)	23 (23.5%)	35 (21.0%)
• Branching	4 (5.8%)	4 (4.1%)	8 (4.8%)
• Granular	3 (4.3%)	5 (5.1%)	8 (4.8%)
Banded	10 (14.5%)	12 (12.2%)	22 (13.2%)
Patchy	4 (5.8%)	3 (3.1%)	7 (4.2%)
Focal	1 (1.4%)	7 (7.1%)	8 (4.8%)
Fovea involvement in fellow eye			
No	48 (69.6%)	77 (78.6%)	125 (74.9%)
Yes	21 (30.4%)	21 (21.4%)	42 (25.1%)
Baseline GA, mm^2			
Mean (SD)	3.92 (4.62)	3.83 (4.94)	3.87 (4.80)
Median [min, max]	2.33 [0.0490, 21.5]	1.99 [0.0490, 29.9]	2.17 [0.0490, 29.9]
Distance from fovea, µm			
Mean (SD)	563 (265)	382 (304)	456 (302)
Median [min, max]	538 [81.0, 1500]	317 [20.0, 1380]	401 [20.0, 1500]
Outer nuclear layer, µm			
Mean (SD)	77.7 (16.8)	72.6 (13.4)	74.7 (15.1)
Median [min, max]	80.0 [44.0, 125]	72.0 [44.0, 100]	75.0 [44.0, 125]
Outer retinal thickness, µm			
Mean (SD)	82.2 (6.12)	82.2 (8.16)	82.2 (7.35)
Median [min, max]	80.0 [67.0, 108]	81.0 [55.0, 113]	81.0 [55.0, 113]
Choroidal thickness, µm			
Mean (SD)	158 (84.4)	162 (82.9)	160 (83.3)
Median [min, max]	137 [50.0, 410]	142 [43.0, 470]	141 [43.0, 470]
Subfoveal drusen			
No	51 (73.9%)	58 (59.2%)	109 (65.3%)
Yes	18 (26.1%)	39 (39.8%)	57 (34.1%)
Subretinal drusenoid deposits			
No	18 (26.1%)	29 (29.6%)	47 (28.1%)
Yes	51 (73.9%)	68 (69.4%)	119 (71.3%)
Refractile drusen			
No	56 (81.2%)	69 (70.4%)	125 (74.9%)
Yes	13 (18.8%)	29 (29.6%)	42 (25.1%)
Double layer sign			
No	39 (56.5%)	69 (70.4%)	108 (64.7%)
Yes	30 (43.5%)	29 (29.6%)	59 (35.3%)
Double layer sign thickness, µm			
Mean (SD)	32.0 (14.6)	37.7 (21.6)	34.8 (18.4)
Median [min, max]	30.0 [9.00, 70.0]	34.0 [15.0, 87.0]	32.0 [9.00, 87.0]
Follow-up, mo			
Mean (SD)	42.8 (28)	55.4 (29)	50.3 (29)
Median [min, max]	38.5 [6, 126]	49 [6, 137]	46 [6, 137]

Mean, standard deviation (SD), median, and range are provided for quantitative variables.

Investigative Ophthalmology & Visual Science

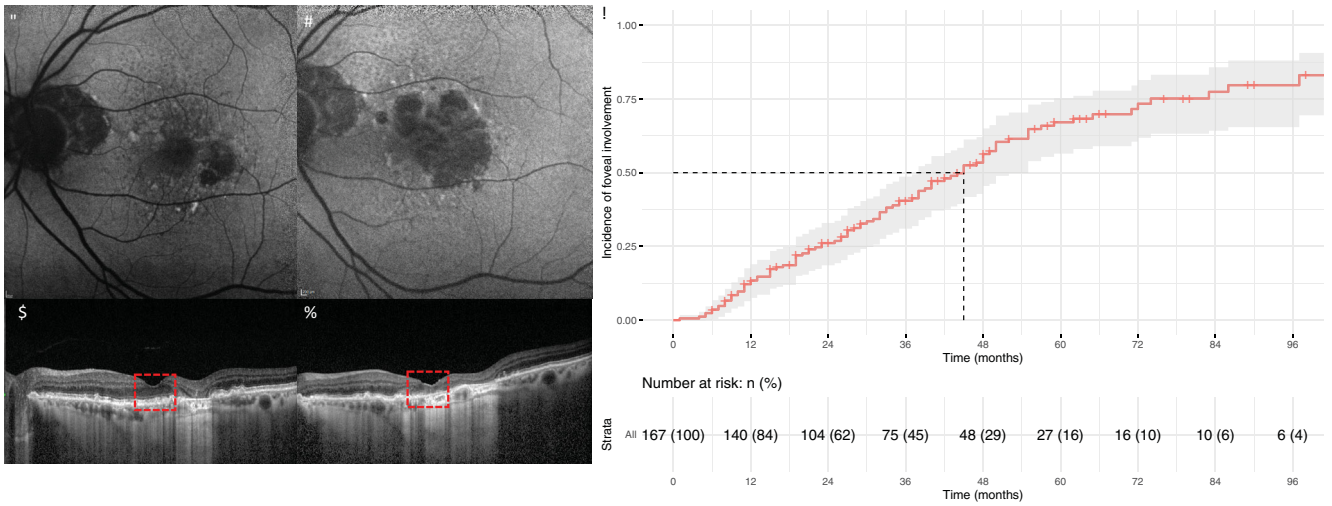

Figure 1. Evolution of foveal involvement in geographic atrophy with initial fovea sparing. (**A**) Baseline blue-light autofluorescence (FAF) imaging displays a small area of decreased FAF superior to the fovea, indicative of early GA changes, accompanied by a diffuse reticular pattern suggestive of underlying subretinal drusenoid deposits. (**B**) Baseline spectral-domain optical coherence tomography (SD-OCT) reveals choroidal hypertransmission and the presence of subfoveal drusen. Importantly, the external limiting membrane (ELM) and ellipsoid zone (EZ) remain intact, and the retinal pigment epithelium (RPE) is preserved, indicating fovea sparing at this stage. (**C**) Follow-up FAF at 4 years demonstrates significant expansion of the hypoautofluorescent area, now encompassing the foveal region, signifying progression to foveal involvement. (**D**) Follow-up SD-OCT at 4 years shows marked outer nuclear layer thinning and ELM descent. Additional features include hyporeflective wedges, disruption of the ELM and EZ, subsidence of the inner nuclear layer and outer plexiform layer, and pronounced choroidal signal hypertransmission within the central 1-mm area beneath the foveal depression, extending over a width of more than 250 µm, confirming foveal involvement. (**E**) Kaplan-Meier curve for foveal involvement illustrates the proportion of patients experiencing fovea involvement over time, with the time measured in months. The *shaded area* represents the 95% confidence interval. The median survival time, where 50% of the study cohort is expected to develop foveal involvement, is *highlighted* on the curve.

Table 2. Cox Proportional Hazards Model Results, Evaluating the Risk Factors Associated With Foveal Involvement in Patients With Geographic Atrophy (GA)

	HR	95% CI	*P* Value
Female gender (ref: M)	0.58	0.26–1.27	0.17
Distance from fovea (for each 10 µm)	0.97	0.96–0.98	<0.001
Baseline GA area (for each 1 mm^2)	1.085	1.01–1.16	0.02
Outer nuclear layer thickness (for each 10 µm)	0.59	0.46–0.74	<0.001
Outer retinal layers thickness (for each 10 µm)	1.70	1.11–2.59	0.01
Double layer sign (ref: no)	0.42	0.20–0.88	0.02
Visual acuity (for each 0.1 LogMAR)	1.37	1.21–1.53	<0.001
Subretinal drusenoid deposits (ref: no)	0.39	0.18–0.84	0.02

Hazard ratio (HR), 95% confidence intervals (CI), and *P* values for various predictors are provided.

Discussion

This study contributes to the literature by scrutinizing risk factors linked to foveal involvement among patients with GA. Through Cox regression analysis, we identified various features significantly influencing the risk of foveal involvement. Advancing our inquiry with a machine-learning algorithm allowed us to measure factors' relative importance, particularly highlighting the critical roles of anatomic proximity to the fovea, baseline VA, and ONL thickness in the progression of GA. Interestingly, although some features like the presence of a DLS and smaller GA area at baseline showed protective traits in traditional analyses, their importance was comparatively less pronounced in more comprehensive models. The presence of significant individual variability still pointed to its inherent complexity and suggests that unmeasured personal characteristics might significantly influence the risk of foveal involvement.

Our findings are in line with previous studies, reinforcing the concept of the fovea's resilience against GA, attributed to its unique anatomic, vascular, and physiological characteristics.[17] This resilience is evident from the foveal sparing rate observed in the Fundus Autofluorescence Imaging in Age-Related Macular Degeneration (FAM) study over a 25-month median follow-up period.[8] Our research, extending over an average of 4 years with a substantial subset of patients monitored for over 5 years, provides a more far-reaching view of foveal involvement incidence. Our results showed slightly lower survival estimates of foveal involvement compared to the Age-Related Eye Disease Study (AREDS) in the initial years (26% vs. 50% at year 2 and 56% vs. 66% at year 4), but aligned more closely in later stages.[18] This discrepancy can likely be attributed to our study's inclusion criteria, particularly the specified minimum size of GA lesions, and the use of OCT in determining foveal involvement as opposed to color fundus photography.

The variability in GA expansion rates underscores the importance of pinpointing reliable biomarkers to predict foveal involvement.[8] In this regard, our study identified the distance from the fovea as a paramount factor. We observed a plateau in the survival curve beyond a certain distance from the fovea, which may suggest a threshold effect, where

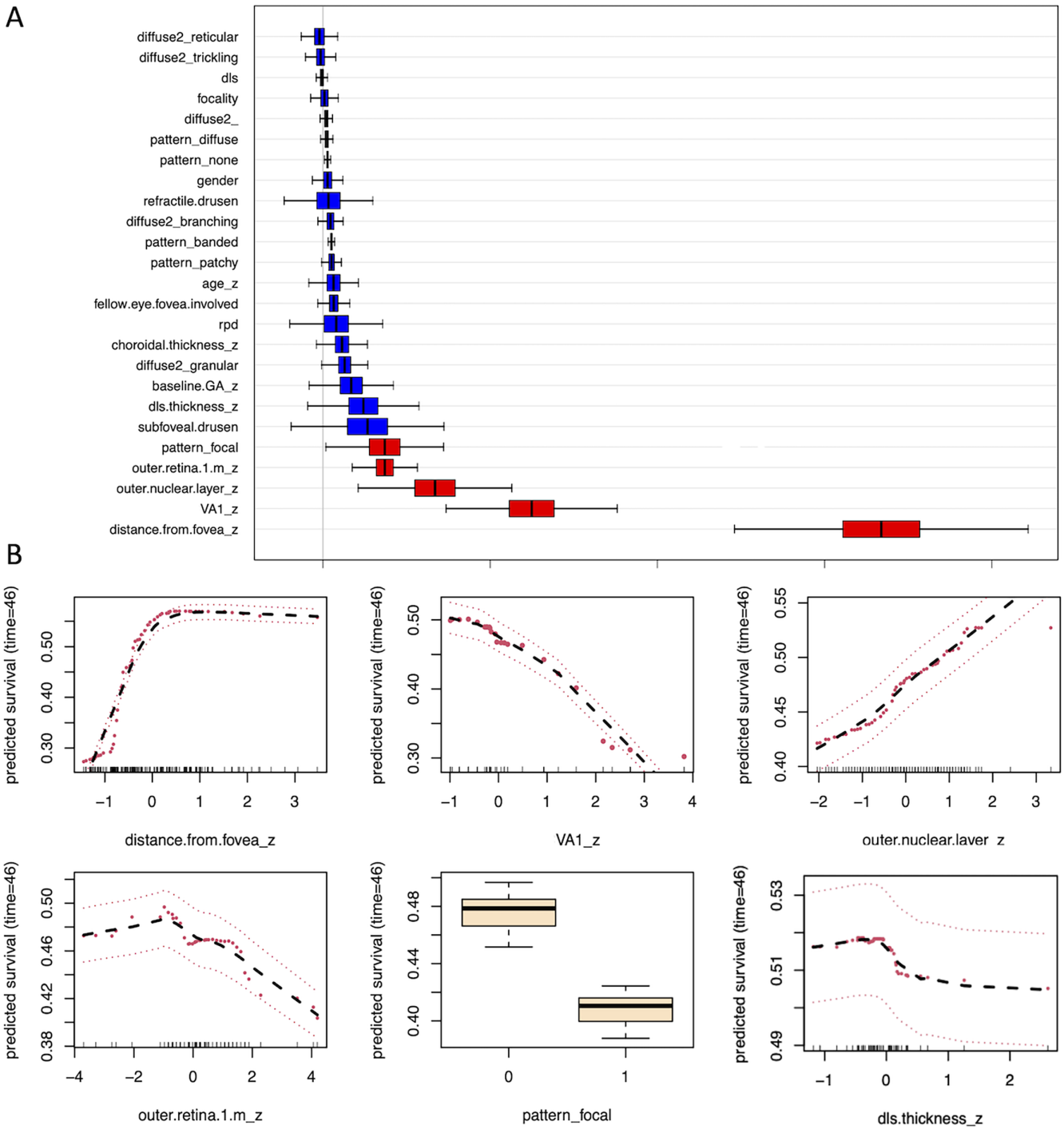

Figure 2. Random survival forest analysis of foveal involvement in geographic atrophy (GA). (**A**) Variable Importance chart delineates the relative importance of various predictors in determining foveal involvement in GA. *Horizontal bars* represent each predictor, arranged in ascending order of their importance. The variables are standardized for quantitative measures and transformed into dummy variables for categorical ones. The most influential factors, including the distance from the fovea, baseline visual acuity (VA), and outer nuclear layer (ONL) thickness, are *highlighted in red* and positioned lower in the chart, underscoring their greater predictive significance. (**B**) Partial Dependence Survival Plots displaying survival probabilities for foveal involvement at the median follow-up of 46 months. These plots are based on significant predictors identified through Random Survival Forest analysis, showcasing how variables such as distance from the fovea, baseline VA, ONL thickness, and double layer sign (DLS) thickness influence the likelihood of progression. For continuous variables, X-axes represent standardized scores (z-scores) for each predictor, facilitating a uniform comparison across diverse measurement scales. Y-axis indicates predicted survival probability, with a value of 0.50 representing a 50% chance of progression to foveal involvement by the median follow-up. *Red points* represent partial dependence values, and *dashed red lines* indicate confidence intervals, which are calculated using deleted jackknife estimators for enhanced accuracy and reliability. Dark tick marks along the x-axis mark the distribution percentiles of each predictor, highlighting the density of data points across the variable's range. Sparse tick marks at the plot boundaries signal areas where interpretations should be made with caution, due to the relatively fewer data points contributing to those regions of the predictor's spectrum. For categorical variables, the impact of different autofluorescence (FAF) patterns on foveal involvement risk is displayed

Investigative Ophthalmology & Visual Science

through boxplots. Focal FAF pattern was associated with a higher risk compared to diffuse pattern. The black solid lines represent the estimated partial values. These plots provide insights into non-linear effects and interactions between predictors and the likelihood of foveal involvement.

the risk of foveal involvement markedly decreases beyond this point. This observation aligns with findings that GA areas closer to the fovea, particularly within the 600 to 1200 µm parafoveal zone, tend to progress more rapidly than GA areas located perifoveally.[19] Nevertheless, we are unable to answer the question of whether we are observing a true biological threshold effect, where GA progression risk indeed stabilizes with increased distance from the fovea, or if our study's duration was insufficient to capture the full spectrum of progression in GA areas significantly distant from the fovea. Our findings should be viewed as preliminary, highlighting a potential area for further longitudinal studies with extended follow-up periods.

VA, commonly used as a primary outcome measure in clinical trials and observational studies, may not always accurately reflect disease progression in GA, especially in its initial stages when the fovea is typically unaffected.[20] Our study, however, underscores the importance of baseline VA as an independent predictor of future foveal involvement. A decline in VA could be indicative of underlying macular lesions that were not the primary focus of our research but are nonetheless significant. These include nascent GA,[21] persistent hyper-reflective defects,[22] or incomplete outer retinal atrophy.[3] Such conditions often precede the manifestation of cRORA and are critical factors to consider in patients with GA who initially present with apparent foveal sparing.[23] Moreover, our study draws attention to the importance of assessing the ONL thickness in the foveal region. A diminished ONL thickness could signal central bouquet dyslamination, a disruption in the structural integrity of the Henle fibers layer, possibly accompanied by RPE dysfunction and a decline in choriocapillaris density.[24]

In eyes with GA, the characteristic hypo-FAF areas signifying RPE loss are typically bordered by varying extents of hyper-FAF. The association of focal FAF patterns with slower rates of GA enlargement and smaller baseline lesion sizes is well-established.[9,25] However, our findings challenge this understanding, demonstrating that focal FAF patterns are associated with an increased risk of foveal involvement. This apparent contradiction may be explained by the presence of focal lipofuscin accumulations, often seen alongside drusenoid pigment epithelial detachments or acquired vitelliform lesions, both of which are prone to evolve into macular atrophy following lesion reabsorbtion.[26,27] It is important to note, yet, that only a small fraction (5%) of the eyes in our study exhibited a focal FAF pattern, which could limit the statistical power of these observations.

Contrastingly, the diffuse trickling pattern typically linked with SDD and faster lesion growth,[28] did not emerge as a significant risk factor for foveal involvement in our analysis. Characterized by centrifugal expansion, this pattern is distinguished by ring- or horseshoe-shaped configurations around the fovea and persistent hyper-reflective material splitting the RPE/BM complex on OCT.[29] The resulting grayish appearance on FAF imaging could potentially mask the actual extent of GA within the fovea, thereby complicating the assessment of its progression. Finally, SDD are more commonly linked with rod dysfunction and scotopic vision impairment,[30] which may contribute to the observed foveal sparing despite the presence of diffuse trickling FAF and SDD.

Recent research in a cohort of 330 eyes with intermediate AMD followed over 2 years has shown that thin DLS significantly increased the risk of developing cRORA.[14] This distinction between thin and thick DLS, based on the layers of reflectivity between the BM and the RPE, is crucial as it points to differing histological characteristics: thin DLS likely represent basal laminar deposits, whereas thicker DLS may indicate the presence of non-exudative MNV.[31] Our analysis, which excluded cases with multilayered DLS, revealed thin DLS as a protective factor against foveal involvement. However, a bi-phasic trend emerged in relation to DLS thickness, suggesting that thicker DLS might exacerbate RPE ischemia and dysfunction, leading to foveal atrophy.[32] This observation was paralleled in the assessment of outer retinal thickness, which includes DLS in its measurement.

Whereas our study sheds valuable light on the progression of GA, it is not without limitations. Its retrospective nature may introduce selection bias, limiting the scope of its findings. The study's focus on a Caucasian patient population in a single center might not be representative of broader, diverse populations. The median follow-up period of 45 months may not sufficiently capture the disease's progression, particularly in slowly progressing cases. Additionally, our method for documenting the onset of foveal involvement—based on the timing of patient visits—might not accurately represent the actual timing of disease progression. One potential source of bias was the differing follow-up times between patients with and without foveal involvement, despite using advanced statistical methods to mitigate this effect. Notably, the study did not explore variations in foveal vascularity, which could have provided further insights into the risk of foveal involvement. Moreover, GA patterns that initiate with early foveal involvement may have been under-represented due to our inclusion criteria. We acknowledge that including cases with GA in the fellow eye may introduce important bias. However, it is important to note that excluding one eye per patient to avoid this confounding would not accurately represent the clinical reality, where bilateral involvement is common. In our analytical approach, we integrated the status of fellow-eye involvement as a covariate to mitigate its confounding effect. The process of standardizing and imputing missing data, although necessary, may introduce biases. Finally, the RSF model, despite its advanced capabilities, faces potential overfitting and requires cautious interpretation and external validation.

In conclusion, our study underscores the significance of proximity to the fovea, thinning of the ONL, and baseline VA as key factors in assessing the risk of foveal involvement in GA. The dual-method analysis not only identifies key risk factors but also elucidates their relative importance and impact on disease progression. These findings may become critical for clinicians in identifying patients at higher risk and devising effective management strategies. Future research, ideally in diverse and multi-center settings, is crucial to validate and expand upon these insights, ultimately enhancing the care and treatment of patients with GA.

Investigative Ophthalmology & Visual Science

Acknowledgments

The authors thank NIDEK TECHNOLOGIES S.R.L. (Via dell'Artigianato 6/A - 35020 Albignasego [P.D.]) for automatic data extraction.

Contributorship Statement: All the authors contributed to the conception or design of the work, the acquisition, analysis, and interpretation of data, drafting of the work, revising it critically for intellectual content. Each of the co-authors has seen and agrees with the way his or her name is listed. This article contains additional online-only material.

Declaration of Generative AI and AI-Assisted Technologies in the Writing Process: During the preparation of this work the authors used chatGPT4 in order to improve readability and language of the manuscript. After using this tool/service, the authors reviewed and edited the content as needed and take full responsibility for the content of the publication.

Disclosure: **M.V. Cicinelli**, None; **E. Barlocci**, None; **C. Giuffrè**, None; **F. Rissotto**, None; **U. Introini**, None; **F. Bandello**, Allergan Inc. Irvine, CA, USA (C); Bayer Shering-Pharma, Berlin, Germany (C), Hoffmann-La-Roche Basel, Switzerland (C), Novartis, Basel, Switzerland (C), Sanofi-Aventis, Paris, France (C), Thrombogenics, Heverlee, Belgium (C), Zeiss, Dublin, CA, USA (C), Boehringer-Ingelheim (C), Fidia Sooft (C), Ntc Pharma (C), Sifi (C)

References

1. Caswell D, Caswell W, Carlton J. Seeing beyond anatomy: quality of life with geographic atrophy. *Ophthalmol Ther*. 2021;10(3):367–382.
2. Colijn JM, Liefers B, Joachim N, et al. Enlargement of geographic atrophy from first diagnosis to end of life. *JAMA Ophthalmol*. 2021;139(7):743–750.
3. Sadda SR, Guymer R, Holz FG, et al. Consensus definition for atrophy associated with age-related macular degeneration on OCT: classification of atrophy report 3. *Ophthalmology*. 2018;125(4):537–548.
4. Riedl S, Vogl WD, Mai J, et al. The effect of pegcetacoplan treatment on photoreceptor maintenance in geographic atrophy monitored by artificial intelligence-based OCT analysis. *Ophthalmol Retina*. 2022;6(11):1009–1018.
5. Pfau M, Schmitz-Valckenberg S, Ribeiro R, et al. Association of complement C3 inhibitor pegcetacoplan with reduced photoreceptor degeneration beyond areas of geographic atrophy. *Sci Rep*. 2022;12(1):17870.
6. Fleckenstein M, Mitchell P, Freund KB, et al. The progression of geographic atrophy secondary to age-related macular degeneration. *Ophthalmology*. 2018;125(3):369–390.
7. Breiman L. Random forests. *Machine Learning*. 2001;45(1):5–32.
8. Lindner M, Boker A, Mauschitz MM, et al. Directional kinetics of geographic atrophy progression in age-related macular degeneration with foveal sparing. *Ophthalmology*. 2015;122(7):1356–1365.
9. Holz FG, Bindewald-Wittich A, Fleckenstein M, et al. Progression of geographic atrophy and impact of fundus autofluorescence patterns in age-related macular degeneration. *Am J Ophthalmol*. 2007;143(3):463–472.
10. Rabiolo A, Sacconi R, Cicinelli MV, et al. Spotlight on reticular pseudodrusen. *Clin Ophthalmol*. 2017;11:1707–1718.
11. Nassisi M, Lei J, Abdelfattah NS, et al. OCT risk factors for development of late age-related macular degeneration in the fellow eyes of patients enrolled in the HARBOR study. *Ophthalmology*. 2019;126(12):1667–1674.
12. Oishi A, Thiele S, Nadal J, et al. Prevalence, natural course, and prognostic role of refractile drusen in age-related macular degeneration. *Invest Ophthalmol Vis Sci*. 2017;58(4):2198–2206.
13. Fukuyama H, Huang BB, BouGhanem G, Fawzi AA. The fovea-protective impact of double-layer sign in eyes with foveal-sparing geographic atrophy and age-related macular degeneration. *Invest Ophthalmol Vis Sci*. 2022;63(11):4.
14. Hirabayashi K, Yu HJ, Wakatsuki Y, et al. OCT risk factors for development of atrophy in eyes with intermediate age-related macular degeneration. *Ophthalmol Retina*. 2023;7(3):253–260.
15. Friedman J, Tibshirani R, Hastie T. Regularization paths for generalized linear models via coordinate descent. *J Stat Softw*. 2010;33(1):1–22.
16. Ishwaran H, Gerds TA, Kogalur UB, et al. Random survival forests for competing risks. *Biostatistics*. 2014;15(4):757–773.
17. Owsley C, Jackson GR, Cideciyan AV, et al. Psychophysical evidence for rod vulnerability in age-related macular degeneration. *Invest Ophthalmol Vis Sci*. 2000;41(1):267–273.
18. Lindblad AS, Lloyd PC, Clemons TE, et al. Change in area of geographic atrophy in the Age-Related Eye Disease Study: AREDS report number 26. *Arch Ophthalmol*. 2009;127(9):1168–1174.
19. Mauschitz MM, Fonseca S, Chang P, et al. Topography of geographic atrophy in age-related macular degeneration. *Invest Ophthalmol Vis Sci*. 2012;53(8):4932–4939.
20. Heier JS, Pieramici D, Chakravarthy U, et al. Visual function decline resulting from geographic atrophy: results from the Chroma and Spectri Phase 3 Trials. *Ophthalmol Retina*. 2020;4(7):673–688.
21. Wu Z, Goh KL, Hodgson LAB, Guymer RH. Incomplete retinal pigment epithelial and outer retinal atrophy: longitudinal evaluation in age-related macular degeneration. *Ophthalmology*. 2023;130(2):205–212.
22. Shi Y, Yang J, Feuer W, et al. Persistent hypertransmission defects on en face OCT imaging as a stand-alone precursor for the future formation of geographic atrophy. *Ophthalmol Retina*. 2021;5(12):1214–1225.
23. Jaffe GJ, Chakravarthy U, Freund KB, et al. Imaging features associated with progression to geographic atrophy in age-related macular degeneration: classification of Atrophy Meeting Report 5. *Ophthalmol Retina*. 2021;5(9):855–867.
24. Li M, Huisingh C, Messinger J, et al. Histology of geographic atrophy secondary to age-related macular degeneration: a multilayer approach. *Retina*. 2018;38(10):1937–1953.
25. Biarnes M, Arias L, Alonso J, et al. Increased fundus autofluorescence and progression of geographic atrophy secondary to age-related macular degeneration: the GAIN study. *Am J Ophthalmol*. 2015;160(2):345–353.e345.
26. Bindewald-Wittich A, Dolar-Szczasny J, Kuenzel SH, et al. Blue-light fundus autofluorescence imaging of pigment epithelial detachments. *Eye (Lond)*. 2023;37(6):1191–1201.
27. Chandra S, Gurudas S, Narayan A, Sivaprasad S. Incidence and risk factors for macular atrophy in acquired vitelliform lesions. *Ophthalmol Retina*. 2022;6(3):196–204.
28. Fleckenstein M, Schmitz-Valckenberg S, Lindner M, et al. The "diffuse-trickling" fundus autofluorescence phenotype in geographic atrophy. *Invest Ophthalmol Vis Sci*. 2014;55(5):2911–2920.
29. Antropoli A, Arrigo A, Bianco L, et al. Quantitative multimodal imaging of extensive macular atrophy with pseudodrusen and geographic atrophy with diffuse trickling pattern. *Sci Rep*. 2023;13(1):1822.

Investigative Ophthalmology & Visual Science

30. Steinberg JS, Fitzke FW, Fimmers R, et al. Scotopic and photopic microperimetry in patients with reticular drusen and age-related macular degeneration. *JAMA Ophthalmol*. 2015;133(6):690–697.
31. Shi Y, Motulsky EH, Goldhardt R, et al. Predictive value of the OCT double-layer sign for identifying subclinical neovascularization in age-related macular degeneration. *Ophthalmol Retina*. 2019;3(3):211–219.
32. Sura AA, Chen L, Messinger JD, et al. Measuring the contributions of basal laminar deposit and Bruch's membrane in age-related macular degeneration. *Invest Ophthalmol Vis Sci*. 2020;61(13):19.

Investigative Ophthalmology & Visual Science